

Chlorhexidine Digluconate Uptake and Release from Alkane-crosslinked Nanocellulose Hydrogels and Subsequent Antimicrobial Effect

Jaka Levanič,^a Ida Poljanšek,^a Viljem Vek,^a Mojca Narat,^b and Primož Oven^{a,*}

Drug release profiles of novel alkane-crosslinked nanocellulose hydrogels were investigated. The common antiseptic compound chlorhexidine digluconate (CHX-DG) was loaded into the nanocellulose hydrogels, and the release kinetics were studied under two different release regimes. The hydrogels were effective at absorbing more than their dry weights of the antiseptic and retaining it during diffusion testing, with more than 60% of the drug retained in the hydrogels. Antimicrobial tests showed sustained antimicrobial activity of the CHX-DG-loaded hydrogels even after the two diffusion tests, which was attributable to non-ionic retention of the CHX-DG within the hydrogel structure.

Keywords: Nanocellulose; Hydrogel; Drug release; Chlorhexidine; Antimicrobial efficiency; *Staphylococcus aureus*, Cytotoxicity, Fibroblasts

Contact information: a: University of Ljubljana, Biotechnical Faculty, Department of Wood Science and Technology, Jamnikarjeva 101, 1000 Ljubljana, Slovenia; b: University of Ljubljana, Biotechnical Faculty, Department of Animal Science, Jamnikarjeva 101, 1000 Ljubljana, Slovenia;

* Corresponding author: primoz.oven@bf.uni-lj.si

INTRODUCTION

Maintaining a clean and, preferably, antiseptic environment in wound treatment is important for proper healing and to minimize complications. Thus, materials in contact with open wounds need to comply with several requirements: They should keep the wound moist while absorbing excess exudate, minimize pain by solvent evaporation and by not strongly bonding with the newly produced tissues, and provide a delivery system for bioactive compounds (Koehler *et al.* 2018). Hydrogels meet these requirements and are promising candidates for wound treatment. With advances in nanocellulose production, nanocellulose-based hydrogels have been under development for use in biomedicine. Initially, bacterial nanocellulose sheets were investigated due to their convenient formation in sheet form and desirable properties such as high water content, biocompatibility, and mechanical stability (Sulaeva *et al.* 2015). More recently, surface-modified nanocellulose has become available, such as 2,2,6,6-tetramethylpiperidine-1-oxyl radical (TEMPO)-modified and carboxymethylated cellulose (Saito *et al.* 2007; Wågberg *et al.* 2008; Naderi *et al.* 2015). Moreover, crosslinking procedures for nanocellulose have opened paths to non-bacterial nanocellulose hydrogels, which can be purified to have very low endotoxin levels (Nordli *et al.* 2019). Coupled with their biodegradability, this property enables nanocellulose hydrogels to be used as temporary 3D matrices for drug delivery within the body and as a topical product (Liu *et al.* 2016). Furthermore, nanocellulose hydrogels, especially those made from TEMPO-oxidized cellulose nanofibrils, are non-cytotoxic and can retard some common wound bacteria (Alexandrescu *et al.* 2013; Liu *et al.* 2016; Powell *et al.* 2016). Additionally, nanocellulose hydrogels have been found to be impermeable to

pathogens in a clinical setting, thus providing a barrier preventing pathogens from infecting a wound (Basu *et al.* 2018).

The diffusion of drugs from nanocellulose matrices has also been studied, to a degree. In some cases, nanocellulose matrices have been found to retard drug diffusion, *i.e.*, yield longer drug release times. For certain types of drugs, such as itraconazole and beclomethasone, drug diffusion from nanofibrillated cellulose (NFC) films follows zero-order kinetics (Kolakovic *et al.* 2012a). It has also been found that the drug diffusion kinetics are governed primarily by electrostatic interactions between the drug and the cellulose matrix, as well as by the molecular size of the drug and the interfibrillar spaces, most notably in dried NFC structures (Kolakovic *et al.* 2012b, 2013) where the structure is essentially nonporous. Research on woven cellulose fabrics treated with chlorhexidine digluconate and NFC dispersions has found that the addition of NFC slows the drug diffusion, while following first-order kinetics (Lavoine *et al.* 2014).

In this study, the drug diffusion properties of novel alkane-crosslinked nanocellulose hydrogels were investigated. By loading these hydrogels with a gold-standard antiseptic molecule, chlorhexidine digluconate (CHX-DG), the release kinetics of this molecule from the crosslinked nanocellulose hydrogels was investigated. Additionally, the antimicrobial activity of the CHX-DG in the crosslinked nanocellulose hydrogels was evaluated, with emphasis on the activity of the residual CHX-DG present in the hydrogels after the release protocol. The antimicrobial activity was checked against a common opportunistic microbe present in surface wounds, *Staphylococcus aureus*, against which CHX-DG is highly effective.

EXPERIMENTAL

Materials

The cellulose used in this experiment was a sulfite-dissolving cellulose pulp (Domsjö Fabriker AB, Örnsköldsvik, Sweden). Sodium hypochlorite was supplied by Acros Organics (Geel, Belgium). Sodium bromide, (2,2,6,6-tetramethylpiperidin-1-yl)oxyl (TEMPO), 1,4-diiodobutane (DIB), 1,10-diiododecane (DID), triiodomethane (TIM), and CHX-DG (20% solution) were supplied by Sigma-Aldrich (Munich, Germany). The solvents used (acetone, dimethyl sulfoxide (DMSO), and ethanol) were of reagent grade and supplied by ECP, d.o.o. (Ljubljana, Slovenia). All reagents and solvents were used as received and without further purification. Distilled water was used in all parts of the experiment, unless noted otherwise.

Gel Preparation

Briefly, never-dried dissolving cellulose was oxidized in a TEMPO-mediated system using sodium hypochlorite and sodium bromide. The procedure has been extensively described in the literature (Saito *et al.* 2007; Isogai *et al.* 2011; Kuramae *et al.* 2014). The oxidized product was subsequently homogenized in a two-stage high-pressure homogenizer until TEMPO-cellulose nanofibrils (TCNF) in the form of a translucent gel were obtained. Water was partially displaced by DMSO, and the crosslinking reaction was performed with 3 crosslinkers (TIM, DIB, and DID) at 90 °C for 24 h. The crosslinked gel samples were cut into 13-mm-diameter discs with a height of 4.5 mm and transferred into an acetone bath for purification. After purification, the acetone was displaced by distilled water in a stepwise procedure, where the acetone content in the gels was gradually lowered.

To remove the residual acetone, the gel pellets were immersed in distilled water and placed in a vacuum chamber at 50 mbar for 1 h and at 25 mbar for 1 h. The purified hydrogel samples were used for further processing.

Cytotoxicity Assay of Alkane Crosslinked Nanocellulose Hydrogels

To test the cytotoxicity of hydrogels the fibroblast cell line NIH 3T3 was used. Cells were cultured in DMEM supplemented with 10% FBS (HyClone) and 1% gentamicin. The 3rd passage of cells was seeded in 6-well plates at a density of 200 cells/well and incubated in 5% CO₂ at 37 °C for 48 h.

A direct contact cytotoxicity assay was performed on the hydrogel samples. Round disc samples (0.95 cm²) of hydrogels were dipped in 0.9% NaCl and autoclaved. Before the direct contact cytotoxicity assay the hydrogels were incubated in fresh cell culture medium for 1 h. After the NIH 3T3 cells were replaced with fresh culture medium, the hydrogel samples, TIM-TCNF, DIB-TCNF, and DID-TCNF (each hydrogel type was tested without and with CHX-DG incorporated into its structure) were placed in each well and incubated for 24 hours in 5% CO₂ at 37 °C. Negative (cells in culture medium) and positive (cells, treated with 0.001% CHX) controls were treated the same way. The viability was checked by standard trypan blue staining. The morphology and viability of cells were observed by inverted light microscope (Nikon Eclipse, Japan) under 100x magnification. The experiment was performed twice.

CHX-DG Loading into Hydrogels and Detection

Hydrogel samples were loaded with CHX-DG (Fig. 1) by soaking them in a standardized solution (2 mg/mL).

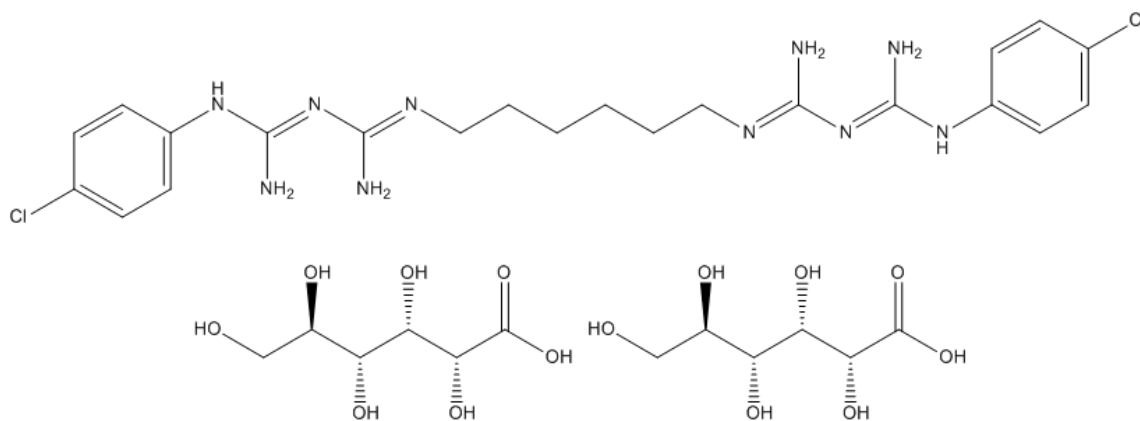


Fig. 1. CHX-DG, containing 15.59% nitrogen, making it easily detectable by elemental analysis

To investigate the loading dynamics *via* diffusion, several parallel samples were prepared. Three hydrogel samples were soaked in 30 mL of the 2 mg/mL solution. Three different loading times were investigated: 24 h, 48 h, and 72 h. Parallels of three samples were analyzed for each hydrogel type, with control samples also present. The control samples comprised three hydrogel pellets soaked in 30 mL of distilled water for each hydrogel type (TIM-, DIB-, and DID-crosslinked). The hydrogel specimens loaded with the CHX-DG were removed from the standardized solution at the 24 h, 48 h, and 72 h marks. They were subsequently freeze-dried (LyoQuest, Telstar, Terrassa, Spain) to obtain their corresponding aerogels. Elemental analysis (Vario PYRO Cube, Elementar

Analysensysteme GmbH, Langenselbold, Germany) of the samples was performed to determine the total nitrogen content, from which the amounts of CHX-DG present in the individual aerogel pellets could be calculated. Great care was taken to quantitatively transfer the samples from their freeze-drying vessels into the tin elemental analysis cups, to obtain an accurate depiction of the total amount of CHX-DG present in an aerogel sample, thus eliminating any concentration gradient, should there have been one within the hydrogel. The amount of CHX-DG present in the samples was calculated using Eq. 1,

$$m_{\text{CHX-DG}} = \frac{m_{\text{Aerogel}} \cdot W_{\text{Aerogel Nitrogen}}}{W_{\text{CHX-DG Nitrogen}}} \cdot 1000 \quad (1)$$

where $m_{\text{CHX-DG}}$ is the mass of CHX-DG present (mg), m_{Aerogel} is the mass of either the control or the CHX-DG-containing aerogel sample (g), and $W_{\text{Aerogel Nitrogen}}$ and $W_{\text{CHX-DG Nitrogen}}$ are the weight fractions of nitrogen contained in the aerogel and the antiseptic, respectively.

Diffusion Profiles of CHX-DG from Alkane-crosslinked Nanocellulose Hydrogels and Its Detection in Solution

The detection of CHX-DG was achieved by ultraviolet-visible (UV-VIS) spectrophotometry (Lambda 2 UV-VIS spectrophotometer, PerkinElmer, Waltham, MA) at the absorption maximum of the biguanide molecule, at 255 nm. Quartz cuvettes were used for the experiment. Prior to the diffusion testing, a UV-VIS calibration curve was prepared with 11 data points, ranging from pure water to 100 $\mu\text{g/mL}$ of CHX-DG in 10- $\mu\text{g/mL}$ increments. The calibration curve had an R^2 value of 0.9991. Diffusion profiles were investigated by two methods to illuminate the behavior under continuous and intermittent release conditions.

In the continuous diffusion experiment, a single hydrogel pellet was soaked in 100 mL of distilled water, and an aliquot of solution was taken at time intervals of 15 min, 30 min, 45 min, 60 min, 90 min, 120 min, 150 min, 180 min, and every full hour after the third hour until 8 h had elapsed. Once taken, the aliquots were analyzed by UV-VIS spectrophotometry at 255 nm and then returned to the main solution. Thus, the volume of solution with the sample was kept constant.

In the intermittent diffusion experiment, a single hydrogel pellet was soaked in 100 mL of distilled water, and an aliquot of solution was taken and analyzed by UV-VIS spectrophotometry as previously described. The liquid medium was then replaced with 100 mL of fresh distilled water. This was repeated every time a sample was taken. Sampling was performed every 30 min until 8 h of total soaking time had elapsed.

Antimicrobial Efficiency on *Staphylococcus aureus*

Antimicrobial testing was performed by placing a hydrogel sample in the middle of a blank agar-filled Petri dish, with an amount of inoculated agar medium poured over the hydrogel pellet. The testing was done according to ISO 22196: Measurement of antibacterial activity on plastics and other non-porous surfaces. The hydrogel samples comprised a blank control sample, a sample loaded with 3.4 mg of CHX-DG, and two samples loaded with CHX-DG after the continuous and intermittent diffusion experiments, both after 8 h of diffusion testing. For each sample type, 3 parallels were tested. The zone of inhibition was measured after 24 and 48 h. Normalized inhibition zones (NW_{Halo}) were calculated according the following formula (2),

$$NW_{Halo} = \frac{d_{iz}-d}{2d} \quad (2)$$

where d_{iz} and d are the diameters of the inhibition zone and hydrogel pellet in millimeters, respectively. The results presented are those of 3 parallel measurements. The *Staphylococcus aureus* strain NCTC 1803 was used in the test.

RESULTS AND DISCUSSION

Cytotoxicity assay of hydrogels

Results of the direct contact method showed that the hydrogels without CHX-DG were not cytotoxic to the tested cell line. The NIH T3T cell line exhibited normal morphology while in direct contact. The impression of flattening of cells under the hydrogels, as observed by optical microscopy, can be attributed to the fact that they have been grown under the constant strain of the hydrogel sample. Cells however, maintained their membrane integrity (Fig. 2A, C and E). Adding CHX-DG had a strongly negative effect on cell viability, as demonstrated by trypan staining (Fig 2B, D and F). The cytotoxicity of the hydrogels is thus governed only by the CHX-DG included within them.

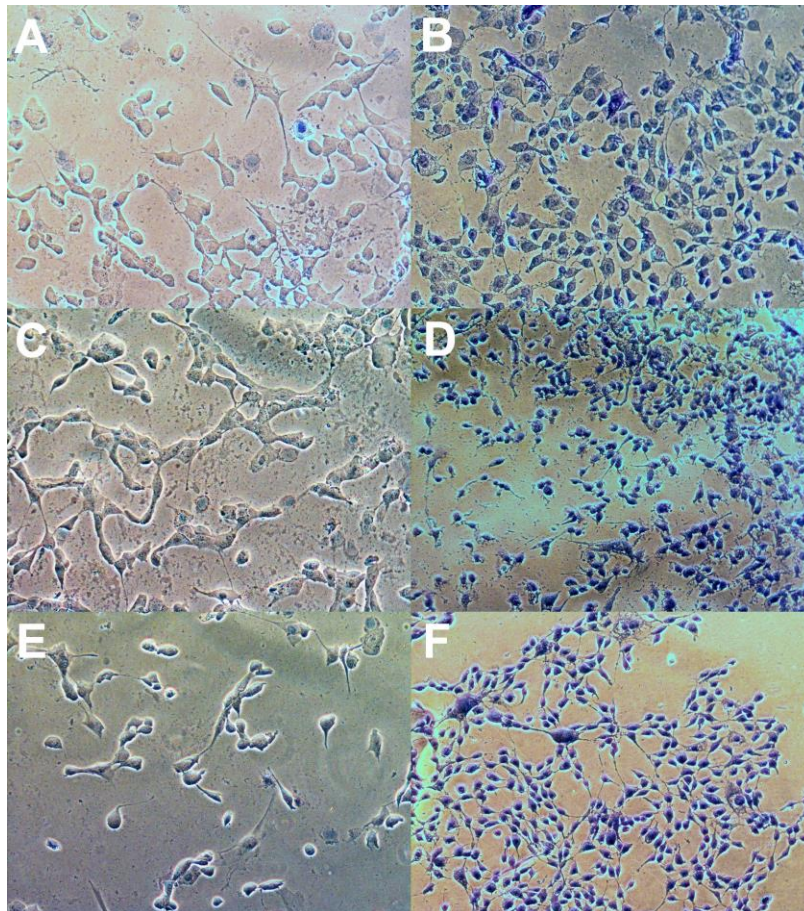


Fig. 2. Light microscopy images of NTC 3T3 fibroblasts in direct contact with the tested hydrogels (100 x magnification). TIM-TCNF samples without and with CHX-DG (A and B), DIB-TCNF hydrogels without and with CHX-DG (C and D) and finally, DID-TCNF samples without and with CHX-DG (E and F), respectively.

Furthermore, no differences between the individual hydrogels could be observed in terms of cytotoxicity related to the used crosslinker, as similar morphology was observed for cells under all tested hydrogels without CHX-DG. Additionally, the negative and positive controls, *i.e.* growth medium and 0.001% CHX-DG supplemented growth medium, exhibited 98% cell viability and 100% cell death, respectively, indicating that CHX-DG is strongly toxic to NIH T3T cells. The cytotoxic effect of CHX and non-cytotoxic nature of nanocellulose hydrogels made from TEMPO oxidized cellulose nanofibrils are corroborated by previous reports (Alexandrescu *et al.* 2013; Liu *et al.* 2018).

CHX-DG Uptake into Crosslinked Nanocellulose Hydrogels

Chlorhexidine digluconate is a cationic bisbiguanide antiseptic; as such, an appreciable amount of nitrogen is present in its structure. Thus, its content in the hydrogels could be effectively determined by analyzing the elemental compositions of the resulting aerogels. Elemental analysis of the control hydrogel samples and the CHX-DG-loaded counterparts showed that there was no nitrogen in the control samples, whereas the CHX-DG-loaded samples had an appreciable amount of nitrogen. In all cases, nearly 10% of the samples were composed of nitrogen, as a result of the CHX-DG's presence (Table 1).

Table 1. Average Carbon, Nitrogen, and CHX-DG Contents in Hydrogels, Neat and after Soaking in the Stock Solution, as Obtained by Elemental Analysis. \pm values presented are standard deviations calculated from 3 measurements

Sample ID	Average Aerogel Mass (mg)	Average C (%)	Average N (%)	Average CHX-DG (mg)
TIM-TCNF (Blank)	2.573 \pm 0.092	41.621 \pm 0.069	0.000 \pm 0.003	0.000 \pm 0.000
TIM-TCNF (24 h)	5.560 \pm 0.065	44.527 \pm 0.188	9.730 \pm 0.096	3.4662 \pm 0.048
TIM-TCNF (48 h)	5.541 \pm 0.013	44.549 \pm 0.050	9.750 \pm 0.032	3.4629 \pm 0.039
TIM-TCNF (72 h)	5.592 \pm 0.041	44.510 \pm 0.093	9.770 \pm 0.014	3.5024 \pm 0.013
DIB-TCNF (Blank)	2.610 \pm 0.037	41.730 \pm 0.059	0.000 \pm 0.002	0.000 \pm 0.000
DIB-TCNF (24 h)	5.384 \pm 0.017	44.523 \pm 0.018	9.820 \pm 0.103	3.3889 \pm 0.039
DIB-TCNF (48 h)	5.455 \pm 0.021	44.469 \pm 0.213	9.810 \pm 0.032	3.4296 \pm 0.081
DIB-TCNF (72 h)	5.477 \pm 0.037	44.541 \pm 0.005	9.820 \pm 0.101	3.4491 \pm 0.065
DID-TCNF (Blank)	2.610 \pm 0.035	38.708 \pm 4.003	0.000 \pm 0.001	0.000 \pm 0.000
DID-TCNF (24 h)	5.377 \pm 0.017	44.490 \pm 0.068	9.640 \pm 0.043	3.3220 \pm 0.024
DID-TCNF (48 h)	5.423 \pm 0.016	44.477 \pm 0.038	9.650 \pm 0.039	3.3528 \pm 0.032
DID-TCNF (72 h)	5.388 \pm 0.028	44.480 \pm 0.031	9.760 \pm 0.108	3.3713 \pm 0.033

The values presented are those of 3 consecutive measurements. TIM-TCNF – TIM-crosslinked hydrogel; DIB-TCNF – DIB-crosslinked hydrogel; DID-TCNF – DID-crosslinked hydrogel

The calculated amounts of CHX-DG were consistent throughout the different hydrogel samples, with values ranging from 3.3 mg to 3.5 mg per hydrogel pellet. Although the hydrogel pellets were soaked for a total of 72 h, by the first sampling point (at 24 h), all the hydrogels had already absorbed almost all of the CHX-DG that they had by the end. Leaving the pellets in the stock solution for 48 h and 72 h had minimal impact on the absorbed amount of CHX-DG, as a plateau had already been reached. Notably, the hydrogels were able to absorb more CHX-DG than their neat dry weight; approximately 2.5 mg of dry hydrogel equivalent was capable of absorbing approximately 3.4 mg of CHX-DG. The effect of different crosslinkers was negligible at best.

Diffusion of CHX-DG from Crosslinked Nanocellulose Hydrogels

The hydrogel pellets were loaded with CHX-DG, and their diffusion profiles were examined under continuous and intermittent conditions. A UV calibration curve was first prepared, with 11 data points taken from 0 $\mu\text{g/mL}$ to 100 $\mu\text{g/mL}$ in 10- $\mu\text{g/mL}$ steps. A linear increase of UV absorption was observed with a coefficient of determination (R^2) of 0.9991. The curve obtained was used for determination of CHX-DG in solution.

Table 2. Percentages of Released CHX-DG from Hydrogels under Continuous Diffusion Conditions

Time (min)	Chlorhexidine Released into Medium (%)		
	TIM-TCNF	DIB-TCNF	DID-TCNF
0	0.00 \pm 0.00	0.00 \pm 0.00	0.00 \pm 0.00
15	12.26 \pm 0.74	10.38 \pm 0.40	11.98 \pm 0.12
30	17.18 \pm 0.59	15.84 \pm 0.78	15.59 \pm 0.38
45	20.78 \pm 0.23	18.63 \pm 0.74	18.43 \pm 0.59
60	23.39 \pm 0.45	21.46 \pm 0.65	20.90 \pm 0.51
90	27.12 \pm 0.59	25.28 \pm 0.85	23.85 \pm 0.65
120	29.03 \pm 0.63	27.82 \pm 1.04	25.93 \pm 0.93
150	31.18 \pm 0.76	29.98 \pm 1.04	27.99 \pm 1.07
180	32.32 \pm 0.64	31.43 \pm 1.44	29.37 \pm 0.88
210	32.44 \pm 0.93	32.82 \pm 1.59	30.07 \pm 1.02
240	33.36 \pm 0.88	33.44 \pm 1.14	30.66 \pm 0.83
300	34.41 \pm 0.78	34.31 \pm 1.61	31.24 \pm 0.99
360	34.82 \pm 0.95	34.83 \pm 1.60	31.99 \pm 1.18
420	34.59 \pm 1.08	35.86 \pm 1.79	32.61 \pm 1.06
480	35.10 \pm 0.93	35.16 \pm 1.67	32.76 \pm 1.03

TIM-TCNF – TIM-crosslinked hydrogel; DIB-TCNF – DIB-crosslinked hydrogel; DID-TCNF – DID-crosslinked hydrogel. \pm values presented are standard deviations calculated from 3 measurements.

Under continuous diffusion, a rapid increase of CHX-DG in solution was observed. Within 120 min, approximately 83%, 77%, and 81% of the total releases had occurred in the TIM-TCNF, DIB-TCNF, and DID-TCNF hydrogels, respectively. After 120 min, the diffusion of CHX-DG slowed, with approximately 2% of the total being released in the next 30 min, for all hydrogel types. The diffusion of CHX-DG nearly ceased after 180 min for the TIM-TCNF hydrogels and after 240 min for the DIB-TCNF and DID-TCNF hydrogels (Table 2). All hydrogels had comparable diffusion profiles, that of a first-order system, in which the release rate depends on the concentration of the drug in the delivery system.

Table 3. Percentages of CHX-DG Released under Intermittent Diffusion Conditions from the Crosslinked Hydrogels

Time (min)	TIM-TCNF		DIB-TCNF		DID-TCNF	
	Average CHX-DG Release per Cycle (%)	Average Cumulative CHX-DG Release (%)	Average CHX-DG Release per Cycle (%)	Average Cumulative CHX-DG Release (%)	Average CHX-DG Release per Cycle (%)	Average Cumulative CHX-DG Release (%)
0	0.00 ± 0.00	0.00	0.00 ± 0.00	0.00	0.00 ± 0.000	0.00
30	16.67 ± 0.59	16.71	16.71 ± 0.76	16.71	14.58 ± 0.56	14.58
60	6.81 ± 0.17	23.52	6.39 ± 0.79	23.10	7.32 ± 0.70	21.90
90	4.07 ± 0.14	27.59	5.20 ± 0.11	28.30	3.97 ± 0.33	25.87
120	1.95 ± 0.26	29.54	2.71 ± 0.13	31.02	2.39 ± 0.08	28.26
150	1.48 ± 0.23	31.02	1.47 ± 0.15	32.49	1.76 ± 0.10	30.02
180	0.35 ± 0.17	31.37	0.97 ± 0.18	33.46	1.43 ± 0.21	31.45
210	0.61 ± 0.32	31.98	0.46 ± 0.18	33.93	1.11 ± 0.26	32.57
240	0.06 ± 0.06	32.04	0.28 ± 0.21	34.21	0.90 ± 0.12	33.47
270	0.00	32.04	0.17 ± 0.21	34.38	0.35 ± 0.12	33.82
300	0.00	32.04	0.09 ± 0.08	34.47	0.11 ± 0.100	33.93
330	0.00	32.04	0.05 ± 0.07	34.52	0.00	33.93
360	0.00	32.04	0.00	34.52	0.00	33.93
390	0.00	32.04	0.02 ± 0.02	34.54	0.00	33.93
420	0.00	32.04	0.00	34.54	0.00	33.93
450	0.00	32.04	0.05 ± 0.04	34.59	0.00	33.93
480	0.00	32.04	0.00	34.59	0.00	33.93

Each washing/release cycle was 30 min, and the medium was renewed for every cycle. TIM-TCNF – TIM-crosslinked hydrogel; DIB-TCNF – DIB-crosslinked hydrogel; DID-TCNF – DID-crosslinked hydrogel. ± values presented are standard deviations calculated from 3 measurements.

The total amount of CHX-DG released did differ among the individual hydrogels. After 8 h, both the TIM-TCNF and DIB-TCNF hydrogels released very similar percentages of CHX-DG: 35.10% and 35.16%, respectively. Meanwhile, the DID-TCNF hydrogels released, on average, only 32.76%. The percentages shown are based on the total amount of CHX-DG present in the hydrogels, as determined by elemental analysis of the aerogels from the same hydrogel batch after soaking in the stock CHX-DG solution for 48 h.

Intermittent diffusion, in which the medium was refreshed after every sampling, also showed an initial burst of CHX-DG into the medium (Table 3). The total cumulative releases of the three hydrogel types were similar in the intermittent diffusion tests. The values after the first cycle (30 min) were in accordance with those of the continuous diffusion experiment after 30 min.

The differences between the hydrogels under continuous and intermittent release conditions seemed negligible at best. All hydrogels released similar amounts of CHX-DG into the medium. This result was surprising, as the concentration gradient was greater when the solvent was renewed, so the intermittent diffusion test was expected to yield higher release amounts from the hydrogels. However, in all cases, the release of CHX-DG ceased after 5 h, or ten 30-min cycles, when no or only miniscule amounts of CHX-DG could be detected (Table 3).

In all hydrogel types, regardless of their respective crosslinkers, a rapid initial increase of CHX-DG was observed in the solvent. All hydrogels also exhibited similar diffusion profiles (Fig. 3). The expectation that different crosslinkers would have an effect on the diffusion kinetics, by affecting the distance between the fibrils, could not be confirmed. By testing three different crosslinkers of varying lengths and functionalities, a slower diffusion, compared to DID-TCNF, was expected for TIM-TCNF and DIB-TCNF, due to the shorter interfibrillar distances. The rates observed during testing, however, were very similar. Crosslink density (using multifunctional crosslinkers with more than two reaction sites) can affect drug diffusion kinetics. Increasing crosslink density decreases the initial burst and prolongs the release of the drug (Martinez *et al.* 2014). Using a short trifunctional crosslinker (TIM) did not affect the diffusion behavior of the tested hydrogels; their behavior was quite similar to their linearly crosslinked hydrogel counterparts (DIB-TCNF and DID-TCNF).

An appreciable portion of the CHX-DG was either irreversibly bound to or trapped within the hydrogel structure. The diffusion studies showed that, in both the continuous and intermittent tests, only approximately 35% of the total CHX-DG was released from the hydrogels. Due to the cationic nature of the antiseptic, it has a strong affinity towards cellulosic materials, even more so for negatively charged cellulose nanofibrils. As is the case with alkane-crosslinked TCNF hydrogels, there remains the potential of unreacted carboxy anion groups being present on the surface of these fibrils, which would undoubtedly attract the positively charged CHX-DG molecules. However, the number of unreacted carboxy groups is small.

It is possible for further negatively charged groups to be present due to residual lignin in the cellulose (Tardy *et al.* 2017). Tests conducted on nanoporous microfibrillated cellulose (MFC) networks have also found that approximately 70% to 75% of chlorhexidine is irreversibly bound to the cellulose network, partly due to negatively charged groups and partly due to hydrogen bonding between the chlorhexidine *p*-chlorophenol and hydroxyl groups on the cellulose (Lavoine *et al.* 2014).

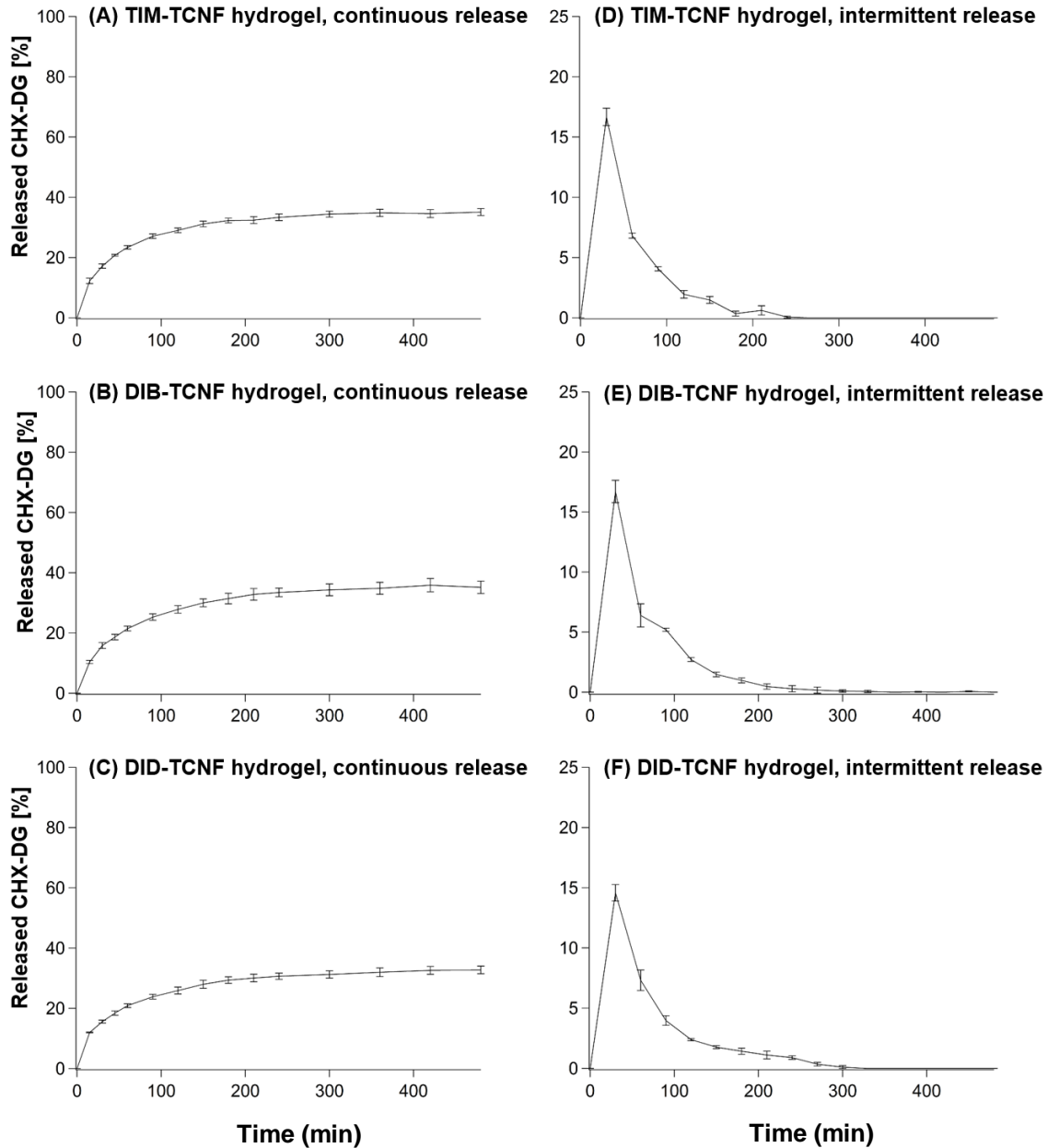


Fig. 3. Graphical representations of release profiles of CHX-DG for different hydrogels under continuous (A, B, and C) and intermittent (D, E, and F) conditions; (A and D) TIM-TCNF – TIM-crosslinked hydrogel; (B and E) DIB-TCNF – DIB-crosslinked hydrogel; (C and F) DID-TCNF – DID-crosslinked hydrogel. The presented values are those of 3 consecutive measurements

Antimicrobial Efficiency

Chlorhexidine digluconate is a powerful antiseptic with a minimal inhibitory concentration (MIC) of 0.625 $\mu\text{g/mL}$ against *Staphylococcus aureus*. It has a total antiseptic activity (TAA) of 1 mg/mL with a contact time of 10 min for complete eradication. Its primary mechanism is interference with the cytoplasmic membranes of target microbes. The biguanide binds to the phospholipids in the membrane, inducing structural modifications and leakage of the intracellular components. Thus, the biguanide group, specifically the cation, is vital to the antiseptic's functionality (Odore *et al.* 2000).

Control samples with no CHX-DG showed no inhibitory activity against *S. aureus*.

The hydrogels showed normal colony presence near and on the hydrogel sample (Fig. 4).

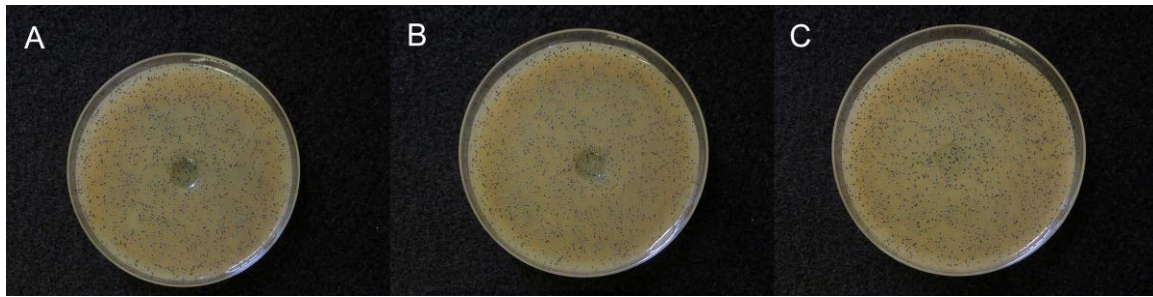


Fig. 4. TIM-TCNF (A), DIB-TCNF (B), and DID-TCNF (C) control samples against *Staphylococcus aureus*, with no CHX-DG loading

Chlorhexidine-loaded samples (approximately 3.4 mg of CHX-DG per hydrogel pellet) showed strong inhibitory action, with an average size of inhibition halos of 17.85 mm, 18.02 mm, and 18.01 mm for the TIM-TCNF, DIB-TCNF, and DID-TCNF, respectively (Fig. 5).



Fig. 5. TIM-TCNF (A), DIB-TCNF (B), and DID-TCNF (C) samples loaded with 3.4 mg of CHX-DG against *Staphylococcus aureus*

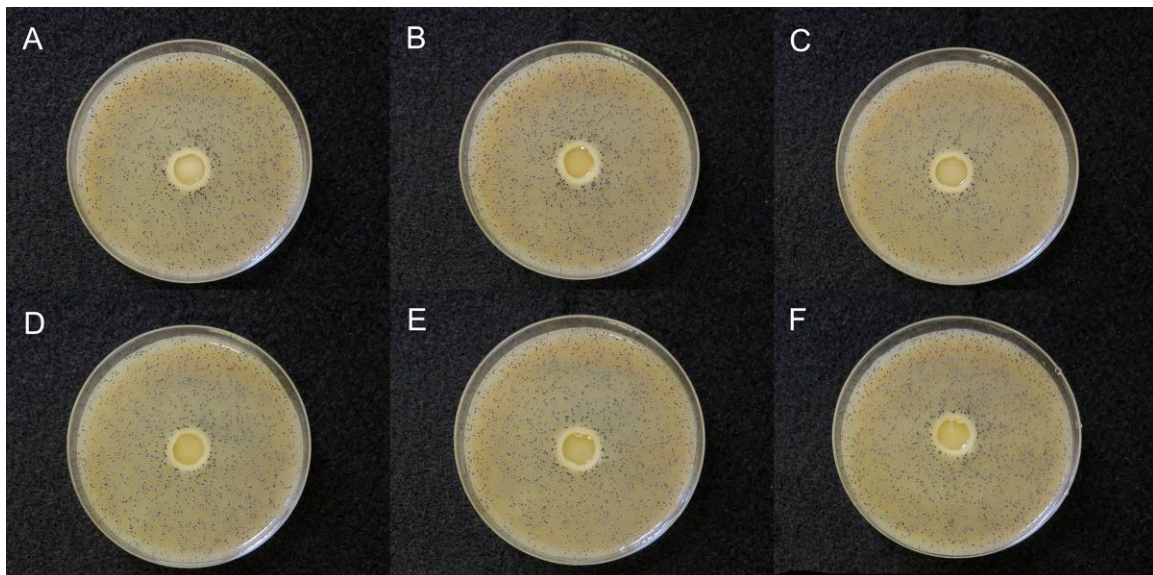


Fig. 6. TIM-TCNF (A), DIB-TCNF (B), and DID-TCNF (C) samples after continuous diffusion experiment and TIM-TCNF (D), DIB-TCNF (E), and DID-TCNF (F) after intermittent diffusion experiments against *Staphylococcus aureus*

After the continuous and intermittent release experiments, the hydrogel samples were also analyzed for their antimicrobial activities (Fig. 5). Under the same conditions, the continuous diffusion samples had inhibition halos of 16.76 mm, 16.33 mm, and 16.66 mm for the TIM-TCNF, DIB-TCNF, and DID-TCNF, respectively. The intermittent diffusion samples performed similarly, with inhibition halos of 16.73 mm, 16.58 mm, and 16.38 mm for the TIM-TCNF, DIB-TCNF, and DID-TCNF, respectively (Fig. 6).

Normalized inhibition zone values were also calculated according to the formula presented in the chapter “Antimicrobial efficiency”. These values are presented in Table 4. A reduction in normalized values can be observed.

Table 4. Inhibition Halo Sizes as Measured in the Petri Dishes and the Standardized Values ($NW_{(halo)}$) Calculated According to Formula 2

Sample ID	Average [mm]	SD [mm]	$NW_{(halo)}$ AVG	$NW_{(halo)}$ SD
TIM CHX	17.85	0.06	0.19	0.01
TIM CDE	16.76	0.15	0.14	0.01
TIM IDE	16.73	0.12	0.14	0.01
DIB CHX	18.02	0.08	0.19	0.01
DIB CDE	16.33	0.22	0.13	0.02
DIB IDE	16.58	0.01	0.14	0.00
DID CHX	18.01	0.06	0.19	0.01
DID CDE	16.33	0.52	0.13	0.01
DID IDE	16.38	0.12	0.13	0.01

The CHX-DG-loaded samples performed well, with a clear inhibition zone, where no bacterial colonies were present. This result agreed with the diffusion experiments, in which approximately one third of the total antiseptic was released into the environment, an amount great enough for TAA. For the continuous and intermittent diffusion samples, no inhibition zone was expected, as per the results of the diffusion experiments. The diffusion of CHX-DG into distilled water ceased after approximately 5 h in the continuous diffusion experiment and after 10 washing cycles in the intermittent diffusion experiment. However, in both cases, an inhibition zone was present, albeit somewhat smaller according to the NW values. It is interesting that an inhibition zone was still present, even though release from the hydrogel pellets ceased. A possible explanation lies in the fact that the growth medium (Baird-Parker agar) has a slightly basic character with a pH value of 7.2, higher than that of distilled water. Further studies would need to be conducted in order to determine the effect of medium pH on the loading and release characteristics of these hydrogels.

Overall, the CHX-DG-loaded hydrogels remained effective in halting the growth of *S. aureus* after both diffusion tests. After the diffusion experiments, because no CHX-DG release was observed after a certain time, it was expected that the CHX-DG was either mechanically trapped within the nanofibrillated cellulose hydrogel structure or bound to the nanofibrillated cellulose hydrogel structure *via* residual presence of carboxy anion. Due to the antimicrobial efficacy of the hydrogel samples after the diffusion experiments, the latter seems unlikely. Having the CHX-DG electrostatically bound to the nanofibrillar structure would undoubtedly inhibit the efficacy of the antiseptic molecule, due to the absence of the cation in the biguanide and its subsequent inability to bind to the phospholipids in the cell walls of the microorganisms. It is more likely that weaker hydrogen bonding occurred *via* the interaction of the *p*-chlorophenol parts of the CHX-DG

and hydroxyl groups on the cellulose. This would allow the antiseptic molecule to retain its antimicrobial properties while limiting its diffusion into the surrounding medium.

CONCLUSIONS

1. The hydrogels themselves show no cytotoxic characteristics. Their cytotoxicity however might be governed by the bioactive compounds contained within them, in our case by the inclusion of CHX-DG
2. Covalently crosslinked nanocellulose hydrogels exhibited first-order diffusion kinetics in distilled water and demonstrated effectiveness as carriers for a model antiseptic compound, CHX-DG.
3. Up to 60% of the total loaded CHX-DG remained in the hydrogels after the continuous and intermittent diffusion tests.
4. Even after the diffusion tests, the hydrogel pellets, which contained residual CHX-DG, exhibited strong inhibition against *Staphylococcus aureus*.

ACKNOWLEDGMENTS

The authors are grateful to Domsjö Fabriker AB (Örnsköldsvik, Sweden) for kindly donating the never-dried dissolving cellulose pulp that was used in this study and to the Slovenian National Laboratory of Health, Environment and Food for assistance with the microbiological testing. Furthermore, we also thank Ana Jakopič from the Biotechnical Faculty, Department of Animal Science for her assistance with cytotoxicity assays. The authors are also grateful to their colleagues from the Laboratory of Stable Isotopes at the Slovenian Forestry Institute, for the elemental analysis. Lastly, the authors also thank the Slovenian Research Agency within the research program P4-0015 and the Ministry of Education, Science and Sport of the Republic of Slovenia for financial support of the “young scientist” programme.

REFERENCES CITED

- Alexandrescu, L., Syverud, K., Gatti, A., and Chinga-Carrasco, G. (2013). “Cytotoxicity tests of cellulose nanofibril-based structures,” *Cellulose* 20(4), 1765-1775. DOI: 10.1007/s10570-013-9948-9
- Basu, A., Heitz, K., Strømme, M., Welch, K., and Ferraz, N. (2018). “Ion-crosslinked wood-derived nanocellulose hydrogels with tunable antibacterial properties: Candidate materials for advanced wound care applications,” *Carbohydrate Polymers* 181, 345-350. DOI: 10.1016/j.carbpol.2017.10.085
- Isogai, A., Saito, T., and Fukuzumi, H. (2011). “TEMPO-oxidized cellulose nanofibers,” *Nanoscale* 3(1), 71-85. DOI: 10.1039/c0nr00583e
- Koehler, J., Brandl, F. P., and Goepferich, A. M. (2018). “Hydrogel wound dressings for bioactive treatment of acute and chronic wounds,” *European Polymer Journal* 100, 1-11. DOI: 10.1016/j.eurpolymj.2017.12.046

- Kolakovic, R., Peltonen, L., Laukkanen, A., Hirvonen, J., and Laaksonen, T. (2012a). "Nanofibrillar cellulose films for controlled drug delivery," *European Journal of Pharmaceutics and Biopharmaceutics* 82(2), 308-315. DOI: 10.1016/j.ejpb.2012.06.011
- Kolakovic, R., Laaksonen, T., Peltonen, L., Laukkanen, A., and Hirvonen, J. (2012b). "Spray-dried nanofibrillar cellulose microparticles for sustained drug release," *International Journal of Pharmaceutics* 430(1-2), 47-55. DOI: 10.1016/j.ijpharm.2012.03.031
- Kolakovic, R., Peltonen, L., Laukkanen, A., Hellman, M., Laaksonen, P., Linder, M. B., Hirvonen, J., and Laaksonen, T. (2013). "Evaluation of drug interactions with nanofibrillar cellulose," *European Journal of Pharmaceutics and Biopharmaceutics* 85(3 Pt B), 1238-1244. DOI: 10.1016/j.ejpb.2013.05.015
- Kuramae, R., Saito, T., and Isogai, A. (2014). "TEMPO-oxidized cellulose nanofibrils prepared from various plant holocelluloses," *Reactive and Functional Polymers* 85, 126-133. DOI: 10.1016/j.reactfunctpolym.2014.06.011
- Lavoine, N., Desloges, I., Sillard, C., and Bras, J. (2014). "Controlled release and long-term antibacterial activity of chlorhexidine digluconate through the nanoporous network of microfibrillated cellulose," *Cellulose* 21(6), 4429-4442. DOI: 10.1007/s10570-014-0392-2
- Liu, J., Chinga-Carrasco, G., Cheng, F., Xu, W., Willför, S., Syverud, K., and Xu, C. (2016). "Hemicellulose-reinforced nanocellulose hydrogels for wound healing application," *Cellulose* 23(5), 3129-3143. DOI: 10.1007/s10570-016-1038-3
- Liu, J. X., Werner, J., Kirsch, T., Zuckerman, J. D., and Virk, M. S. (2018). "Cytotoxicity evaluation of chlorhexidine gluconate on human fibroblasts, myoblasts, and osteoblasts." *J. Bone Jt. Infect.* 3(4), 165-172.
- Martinez, A. W., Caves, J. M., Ravi, S., Li, W., and Chaikof, E. L. (2014). "Effects of crosslinking on the mechanical properties, drug release and cytocompatibility of protein polymers," *Acta Biomaterialia* 10(1), 26-33. DOI: 10.1016/j.actbio.2013.08.029
- Naderi, A., Lindström, T., Sundström, J., Pettersson, T., Flodberg, G., and Erlandsson, J. (2015). "Microfluidized carboxymethyl cellulose modified pulp: A nanofibrillated cellulose system with some attractive properties," *Cellulose* 22(2), 1159-1173. DOI: 10.1007/s10570-015-0577-3
- Nordli, H. R., Pukstad, B., Chinga-Carrasco, G., and Rokstad, A. M. (2019). "Ultrapure wood nanocellulose—Assessments of coagulation and initial inflammation potential," *ACS Applied Bio Materials* 2(3), 1107-1118. DOI: 10.1021/acsabm.8b00711
- Odore, R., Colombatti Valle, V., and Re, G. (2000). "Efficacy of chlorhexidine against some strains of cultured and clinically isolated microorganisms," *Veterinary Research Communications* 24(4), 229-238. DOI: 10.1023/a:1006442715761
- Powell, L. C., Khan, S., Chinga-Carrasco, G., Wright, C. J., Hill, K. E., and Thomas, D. W. (2016). "An investigation of *Pseudomonas aeruginosa* biofilm growth on novel nanocellulose fibre dressings," *Carbohydrate Polymers* 137, 191-197. DOI: 10.1016/j.carbpol.2015.10.024
- Saito, T., Kimura, S., Nishiyama, Y., and Isogai, A. (2007). "Cellulose nanofibers prepared by TEMPO-mediated oxidation of native cellulose," *Biomacromolecules* 8(8), 2485-2491. DOI: 10.1021/bm0703970
- Sulaeva, I., Henniges, U., Rosenau, T., and Potthast, A. (2015). "Bacterial cellulose as a material for wound treatment: Properties and modifications. A review,"

- Biotechnology Advances* 33(8), 1547-1571. DOI: 10.1016/j.biotechadv.2015.07.009
- Tardy, B. L., Yokota, S., Ago, M., Xiang, W., Kondo, T., Bordes, R., and Rojas, O. J. (2017). "Nanocellulose–surfactant interactions," *Current Opinion in Colloid & Interface Science* 29, 57-67. DOI: 10.1016/j.cocis.2017.02.004
- Wågberg, L., Decher, G., Norgren, M., Lindström, T., Ankerfors, M., and Axnäs, K. (2008). "The build-up of polyelectrolyte multilayers of microfibrillated cellulose and cationic polyelectrolytes," *Langmuir* 24(3), 784-795. DOI: 10.1021/la702481v

Article submitted: August 14, 2019; Peer review completed: November 9, 2019, Revised version received: February 10, 2020; Accepted: March 17, 2020; Published: March 27, 2020.

DOI: 10.15376/biores.15.2.3458-3472